Impact of 1D vs 3D Earth Conductivity Based Electric Fields on Geomagnetically Induced Currents

Komal S Shetye, Adam B Birchfield,
Raymund H Lee, Thomas J Overbye
Dept. of Electrical and Computer Engineering
Texas A&M University, College Station, TX, USA
{shetye, abirchfield, lee32982, overbye}@tamu.edu

Jennifer L Gannon
Computational Physics Inc.
Boulder, CO, USA
gannon@cpi.com

***Abstract*—Electric fields that drive geomagnetically induced currents (GICs) depend on the deep earth conductivity. In a power system GIC study, the model used to represent this conductivity thus influences the GIC results. In this paper, we evaluate the differences between the commonly used 1D conductivity model and the more complex 3D transfer functions, in terms of their impact on simulated GICs, by validating them against actual GIC measurements. The goal is to provide illustrative results on the performance of these models, in order to show the present capabilities and areas for improvement of conductivity models, and power system GIC modeling. The paper highlights the importance of data availability for model validation research, in order to mitigate the GMD risk.**

***Index Terms*-- geomagnetically induced currents, geomagnetic disturbance, GIC, GMD, earth conductivity, 1D layered, EMTF**

I. Introduction

Building resilience in power grids against severe geomagnetic disturbances (GMDs) requires modeling and analysis that goes beyond power systems. Geomagnetically induced currents (GICs) can cause blackouts due to a voltage collapse in the grid, as well as transformer heating and damage, among other system issues. The geoelectric (electric) fields induced at the earth's surface due to GMDs are the main driver of GICs. These electric fields depend on 1) the rate of change of magnetic field experienced at a location, and 2) the deep earth conductivity at that location [1], [2]. The earth's conductivity response is frequency dependent.

So far for most power system studies, typically a uniform conductivity model, or a layered 1D model with different conductivity values at different depths, have been used. The geophysics literature describes other more detailed methods of calculating electric fields. One of them is using the electromagnetic transfer functions (EMTFs) approach that represents the 3D conductivity response of the earth. Recently, there has been a persisting question in industry and academia regarding the appropriate conductivity model to be used to calculate electric fields, from a power systems perspective. However, to the authors' best knowledge, there is currently a lack of studies that address this question.

This work is supported by the National Science Foundation (NSF) under Award Number NSF 15-20864, and Bonneville Power Administration under TIP 359: Improved System Modeling for GMD and EMP Assessments.

In this paper, we investigate the impacts of using electric fields derived from 1D versus 3D conductivity structures on simulated GICs. These results are compared for validation purposes with transformer GIC measurements. These were collected from two utility footprints, which have disparate geophysical characteristics, during actual GMD events. The goal of these comparisons and validation is to determine how the 1D and 3D perform against one another for the given scenarios, and if they are comparable then perhaps the simpler 1D model may suffice for system studies and event recreations. We use different metrics to compare, and observations are made recognizing that there are several uncertainties in modeling the GMD phenomenon.

The paper is organized as follows. Section II gives a brief background on the GMD model used in power system studies, followed by descriptions of the 1D and 3D conductivity models that are the focus of this paper. Section III describes case studies of two actual utility footprints. Both simulation results using the two conductivity models, as well as transformer GIC measurements are discussed in this Section. Section IV expands on the geophysical explanations behind the results. Section V summarizes the key findings, with directions for ongoing and future work.

II. GIC Model and Earth Conductivity

A. GIC and Electric Fields

A GMD induces an electric field at the earth. This in turn induces a dc voltage in each of the transmission lines. To calculate this voltage, U_k, induced in line k, the electric field, $\overline{E}$, is integrated over the length of the line [3], [4], [5] as,

$$U_k = \int_{\Re} \overline{E} \cdot \overline{dl} \tag{1}$$

where $\Re$ is the geographic route of the line, and $\overline{dl}$ is the incremental line segment. This expression works for non-uniform electric fields, which is the case with 1D conductivity and 3D EMTF based electric fields.

For a uniform electric field, U_k can be found as,

$$U_k = E_N L_{k,N} + E_E L_{k,E} \tag{2}$$

978-1-5386-4505-5/18/$31.00 ©2018 IEEE

where E_N and E_E are the northward and eastward electric fields, respectively, in V/km. $L_{k,N}$ and $L_{k,E}$ are northward and eastward line lengths, each in kms.

The dc voltage induced on each line *k*, located between buses *l* and *m*, can be converted into its Norton equivalent current injection at bus m by,

$$I_{lm} = I_k = U_{lm} / R_{lm} = U_k / R_k \tag{3}$$

Where R_{lm} (R_k) is the effective series resistance accounting for the dc resistance of transmission line, transformer windings, and substation grounding between those buses [6]. Substituting (2) in (3), we can find the total current injection at a bus *l* by summing up the currents on each of the lines as,

$$I_l = \sum_k \left(\frac{L_{k,N}}{R_k} E_N + \frac{L_{k,E}}{R_k} E_E \right) \tag{4}$$

A vector $\mathbf{I}^{inj}$ is then created from these total current injections at each bus, such that $\mathbf{I}^{inj} = \mathbf{CE}$. **C** depends on the length, orientation, and resistance of the lines.

The nodal dc voltages [7] as a result of these current injections are found as,

$$\mathbf{V} = \mathbf{G}^{-1}\mathbf{I}^{inj} \tag{5}$$

where matrix **G** is similar in form to the power flow admittance matrix, but contains only conductance values and is augmented to include substation neutrals as nodes, and substation grounding conductance values [8]. Solving (5) yields us the GIC flow throughout the system, including transmission lines and through transformer and substation neutrals.

Reference [9] derives a relationship between transformer GICs and the driving electric field, which is summarized below. For a uniform electric field, this relationship is linear, and is given by,

$$\mathbf{I} = \mathbf{JE} \tag{6}$$

where **I** is a vector of the transformer neutral GICs, and **J** is a coefficient matrix which depends on **G** and **C**, and relates GICs to the electric field through some constant coefficients [9]. In other words, **J** depends on the network topology and resistance values. Note that the expression in (6) is applicable mostly to a uniform electric field case, but this concept is introduced here as background for an example discussed further in the paper.

In order to validate simulated GICs with actual GIC measurements obtained from GIC measuring devices (GIC monitors), such as those installed in transformer neutrals, the GIC vector **I** is converted into a matrix **Y** as follows,

$$\mathbf{Y} = \begin{bmatrix} y_1^{t1} & y_1^{t2} & \cdots & y_1^{tT} \\ y_2^{t1} & y_2^{t2} & \cdots & y_2^{tT} \\ \vdots & \vdots & \ddots & \vdots \\ y_P^{t1} & y_P^{t2} & \cdots & y_P^{tT} \end{bmatrix} \tag{7}$$

where each row represents a unique GIC monitor, with a total of *P* such monitors, and each column is a time point, up to the end time *T*. The electric field, calculated from the observed magnetic field, can be expressed as a matrix **X**, with a total of *T* columns and two rows, one for northward and one for the eastward component. Similar to (6), we can express the measured GICs as,

$$\mathbf{Y} = \mathbf{JX} + \mathbf{N} \tag{8}$$

where matrix **N** accounts for measurement noise. It is well known that there are uncertainties in the GMD model; e.g. the exact values of the substation grounding resistances are not known. To account for these, [9] proposes a modified model which includes a scaling factor for each GIC measurement, which can be put together in a diagonal matrix **S** to change (8) to

$$\mathbf{Y} = \mathbf{SJX} + \mathbf{N} \tag{9}$$

The significance of this idea of GIC measurement scaling is illustrated further in the paper.

B. 1D Conductivity Model

So far, we discussed the dc model of a power system, which is used to calculate GICs from the electric fields that drive them. The underlying electric fields are a function of the rate of change of magnetic field, and the deep earth conductivity. This is because these electric fields can penetrate deep into the earth, and are a function of the skin depth, which can range from few kilometers to 100's of km [10]. Hence, one needs to know how the earth's resistivity varies laterally and with the depth. This is commonly referred to as the 1D layered earth model, shown in Figure 1. Figure 2 shows the lateral variations in resistivity, or "conductivity zones", with respect to physiographic regions of the continental US. The conductivity details of each zone are given in [12].

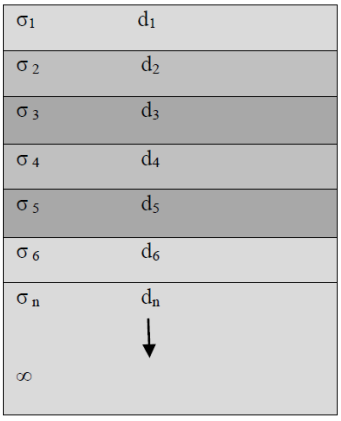

Figure 1. 1D Layered Earth Conductivity Model as depicted in [11]

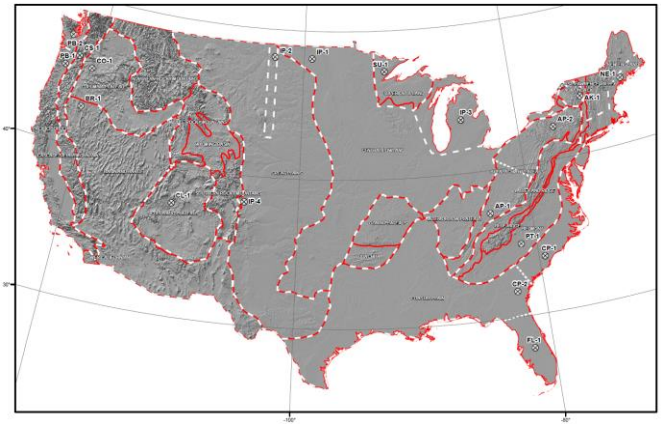

Figure 2. Location of 1D Earth Resistivity Models with respect to Physiographic Regions of the US as shown in [10]

From the layered 1D data, the impedance Z at the surface of the earth is calculated using recursive relations, similar to the concept of transmission line theory, in that each layer is represented by its propagation constant [11]. The impedances are frequency dependent and their selection to calculate the electric fields depends on factors such as sampling rate of the magnetic data, and duration of the data used.

Finally, the electric field is calculated from this earth surface impedance and an estimated magnetic field intensity, as follows,

$$E_x(\omega) = Z_{rg}(\omega) H_y(\omega) \tag{10}$$

$$E_y(\omega) = -Z_{rg}(\omega) H_x(\omega) \tag{11}$$

where $E_x(\omega)$ is the northward electric field (V/m), $E_y(\omega)$ is the eastward electric field, $H_x(\omega)$ is the northward magnetic field intensity (A/m), $H_y(\omega)$ is the eastward magnetic field intensity, and $Z_{rg}(\omega)$ is the earth surface impedance of a region "*rg*" such as the ones shown in Figure 2, all at a frequency ω.

In a given 1D region, which can span upwards of tens of thousands of sq. miles, the E_x and E_y values remain the same at a certain point in time, thus acting like a "uniform" electric field region. Non-uniformities occur when a transmission line crosses two or more 1D zones.

C. 3D Conductivity Model

The 3D conductivity model used here is based on the NSF Earthscope project, which consists of a library of magnetotelluric (MT) measurements made over a large portion of the US [14]. At each measurement location, magnetic and electric fields were recorded over a period of time, which were then transformed into frequency-dependent transfer functions (EMTFs). The EMTFs can be used to derive electric fields at the earth's surface from the magnetic field, and are publicly available through IRIS [15], [16]. Figure 3 shows the array of EMTF locations as of 2017.

Analogous to (10) and (11), the electric field at each EMTF location can be calculated using the estimated magnetic field at that location as follows,

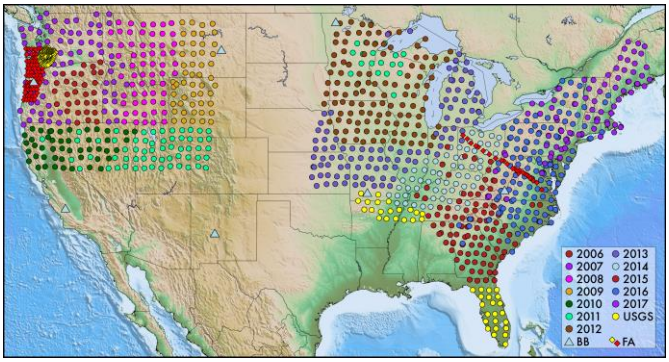

Figure 3. NSF Earthscope Magnetotelluric (MT) Array from [13]

$$\begin{bmatrix} E_x(\omega) \\ E_y(\omega) \end{bmatrix} = \begin{bmatrix} \xi_{xx}(\omega) & \xi_{xy}(\omega) \\ \xi_{yx}(\omega) & \xi_{yy}(\omega) \end{bmatrix} . \begin{bmatrix} B_x(\omega) \\ B_y(\omega) \end{bmatrix} \tag{12}$$

where B is the magnetic field, and ξ is the surface impedance. Since these EMTF locations are unevenly spaced, we interpolate to re-grid over the region of interest, for each time step. The end result is a "data cube" where one dimension is time at 10 second resolution (typically), and the other two are latitude and longitude making a 0.5 degree spatial grid. Reference [17] shows examples of such electric fields estimated for historical and artificial GMD events, and their application to a system model to calculate and compare peak GICs for an actual system in the Pacific Northwest. In the next section, we validate these models with GICs measured during two GMD events in two utility footprints.

III. Case Studies

The two footprints used in the analysis (hereafter referred to as System A and System B) are utility territories in two geographically and physiographically different regions of the US. Names and specific locations have not been disclosed in the paper for confidentiality. System A lies in the western part of the US, whereas System B is in the east. Due to the presence of more granular measurements in [12], System A covers four different 1D zones, while System B is primarily composed of one 1D conductivity zone. The goal behind choosing these two systems is also to evaluate the impact on the simulation results of the more granular 1D data available for System A, as compared to System B.

Ideally, one would compare the same GMD event at a point in time across both these footprints to reduce the variation in the GMD characteristics. However, data is not always readily available to researchers to make such cross-system studies for the same event more prevalent. Not only are moderate to strong GMD events that actually produce perceivable GICs infrequent, measurements and power system models are often hard to acquire due to power system critical energy/electric information infrastructure (CEII) concerns. Hence, the strategy adopted in this paper is to make the best possible use of the available data, and to be cognizant of the fact that these are two different events with different signatures, while making conclusions. For this analysis, we used data available from a GMD event that occurred in May

2016 for System A, while for System B the data corresponds to a GMD event from June 2015.

The general procedure remains the same in both the system studies. The imminent occurrence of a GMD, and further measurements and forecasts once it begins on the earth is predicted and announced by agencies such as the Space Weather Prediction Center (SWPC). This also serves as alerts to radio, satellites, and recently power grid operators due to the harmful impacts GMDs can have on them. Magnetometer observatories and stations present around the globe take measurements of the changing magnetic field, which are stored for posterity. In the power grid, several utilities have installed GIC monitors in transformer neutrals, which can be hall-effect transducers that measure dc current. These can also serve as alerts, as well as be useful for post event analysis. A typical GMD event lasts about 2-3 days.

Once the event has passed, the power system data needed to perform a validation study i.e. 1) the dc network characteristics, and 2) GIC measurements, is collected. We then need the magnetic field data corresponding to the GMD event from one or more magnetometers that are reasonably close to or ideally in the system under study. Some of this data is publicly available. Given the sparsity of the available magnetometer network, interpolation has to be used often to estimate the magnetic field at a location. This is then subjected to an appropriate conductivity profile, similarly to (10), (11) or (12) to calculate the input electric field and subsequently the GICs in the power system, following (1) and (5). The GICs simulated using 3D electric fields shown in this paper are based on EMTFs downloaded on January 30, 2018. This is an important note since results may change with time as more EMTF data becomes available, or gets updated.

A. System A – May 2016 Event

This GMD event occurred on May 8, 2016. We use measurements from two transformers, available at 2 sec. resolution (sampled every five time steps). For anonymity, the transformers are referred to as T1 and T2 here. The remaining transformers had data issues such as dropped packets, zero values, noise, etc. Figure 4 shows comparisons between the magnitudes of the measurements and the simulated GICs using 1D conductivity (top), and 3D EMTF (bottom). This is during the most active part of the storm (23:00 to 05:00 UTC) when the GMD electric field as well the GICs at T1 reached their peak. Figure 5 zooms into the hour of the peak GIC, i.e. 01:00 to 02:00 UTC.

The figures also contain two comparison metrics. CC refers to the Pearson's correlation coefficient, which is defined as,

$$CC = \frac{n\left(\sum \alpha\beta\right) - \left(\sum \alpha\right)\left(\sum \beta\right)}{\sqrt{\left[n\sum \alpha^2 - \left(\sum \alpha\right)^2\right]\left[n\sum \beta^2 - \left(\sum \beta\right)^2\right]}} \qquad (13)$$

where α is the measurement, β is the simulated GIC, and n is the number of time points. L2 norm is a simple Euclidean distance. The former is meant to understand time/phase differences, whereas the L2 norm is more effective for a point-wise magnitude comparison.

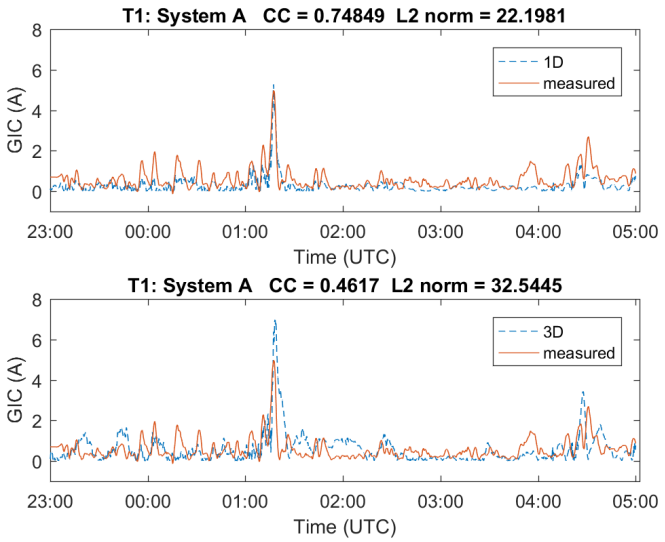

Figure 4. Simulated and Measured GICs at T1. Magnitudes may appear slightly different compared to Figure 5 due to 1) filtering of measurements and 2) plotting artefacts especially with dashed curves.

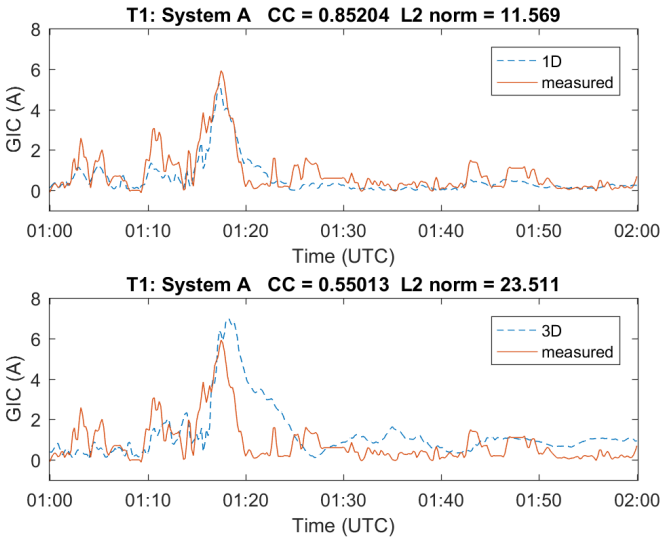

Figure 5 Zoomed in Simulated and Measured GICs at T1

Since multiple measurements (~10) were available from each system, in the interest of space constraints and providing a meaningful discussion, the criteria for choosing the GICs to show in this paper was that at least one of the models, 1D or 3D, should have a CC greater than 0.5, in addition to reasonable data quality. Figures 4 and 5 indicate a good correlation for the 1D results with the actual GICs, along with peak GIC value. Though the CC is relatively low, we see that the 3D is able to capture the overall trends of the actual GIC, but falls short in phase and magnitude at times. Note how the correlations increase for both the 1D and 3D response when we focus on the most active part of the GMD storm.

T2 was another transformer that had promising measurements in terms of quality (i.e. not too noisy, significant magnitude, etc.) from System A. Figure 6, however, shows a very big mismatch between both the 1D

and 3D results, and the measured value. Nonetheless, the CC's were large enough to warrant further investigation.

First, there was an obvious zero error in the measurement, which was corrected. Next, to visualize the two GICs on the same scale, the measurement was scaled down. This was also done in light of the measurement scaling mentioned in (9). While the scaling factor can be found automatically using the approach in Section II, here a trial and error method was used by a simple visual inspection, since the purpose was just to visualize the results on a comparable scale. The scaling factor used here was 1/6 whereas the zero error can be considered as noise, in (9). Figure 7 is what was obtained after applying these two changes. It helps give a better sense of how well the simulation results are actually correlated. It also shows that the zero error correction and the scaling in fact improved the CC of the 3D response over the 1D, with the 1D changing from 0.6 to 0.73 and the 3D CC improving from 0.56 to 0.81.

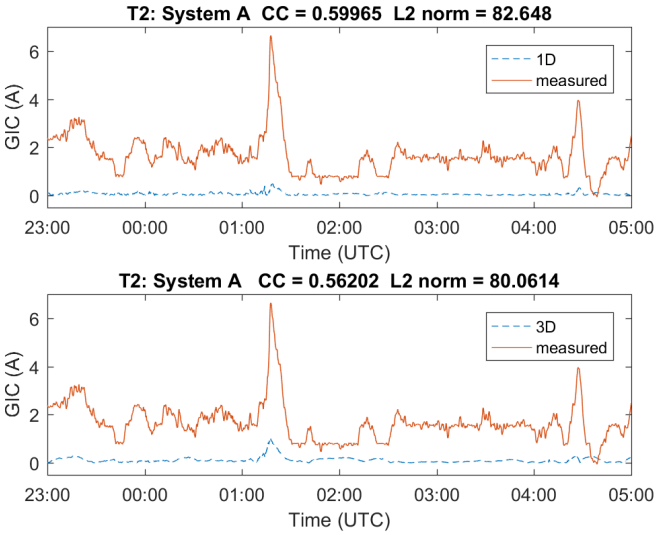

Figure 6. Simulated and measured GICs at T2

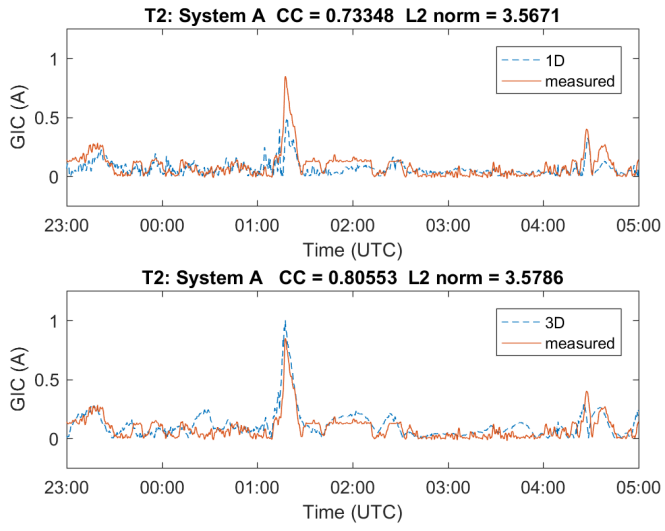

Figure 7. Scaling of measured GICs at T2 by a factor of 6

It is interesting to note though the scaling was derived for a uniform electric field case, applying it to the GIC simulated by the non-uniform 3D electric field also improved its correlation with the measurement. The simulated GICs here are quite low compared to the actual values, pointing to the need for correcting some parameter(s) in the model. The similar values of correlation for the 1D and 3D models could indicate that their structures are similar in this region, and the GIC error is arising from uncertainties in the power system model (resistances, topology, etc.) Finally, the overall better correlation of T1 simulated GICs over T2 could be that the magnetometer used for this study happened to be very close to T1. There was only one magnetometer in this footprint.

B. System B – June 2015 Event

As mentioned earlier, this utility footprint lies in the eastern part of the US. It is also at a more southern latitude than System A. Geomagnetic activity tends to concentrate at higher latitudes near the magnetic poles, hence they typically experience greater GMD effects. The magnitudes of neutral currents in this event, however, were twice of that of System A. This was a major event with significant GICs recorded in some systems, but no damages or blackouts were reported. There was no magnetometer installed yet in this footprint when this storm occurred, hence the magnetic field data for this study was taken from the nearest possible observatory, which is still around 500 miles away from the central part of System B. As mentioned earlier, this footprint is primarily covered by a single 1D region. We expect to see the impacts of these factors in the simulation results.

We again focus on the peak period of the storm, which occurred between 18:30 and 19:00 UTC on June 22, 2015. Figure 8 and Figure 9 show GIC magnitude comparisons from transformers T3 and T4. T3 was the transformer with the largest recorded GICs for this event in System B. For T3, neither of the models are that well correlated as in System A. However, we see that 1D tracks the rise of the GIC towards the peak nearly in phase. Overall, both 1D and 3D get the magnitudes somewhat correct, with issues in the phase.

A slightly better correlation of 0.68 is seen at T4 in the 1D case, compared to T3, which was 0.66. The 3D response is much worse in this case. The rest of the transformers, not shown here, had even lower correlations. There could be two factors contributing to this: 1) the effect of the magnetometer distance from the system making the magnetic field input for the electric field calculations inaccurate, 2) the conductivity structures. The beginning of this Section talked about how System B is primarily covered by one 1D conductivity zone compared to System A that is described by four zones. The overall lower correlations observed for the 1D results compared to System A here could be related to the granularity of the 1D zones, pointing to the need for more measurements to create more conductivity zones in this region. In addition, the overall poor correlations for both models compared to System A can be attributed to the magnetic field input, i.e. the magnetometer being relatively far away from the footprint. In addition, the fact this utility is located near the southeastern

part of the country, where the impact of GICs is often debated, such results further highlight the need to not neglect the assessment of the GIC hazard in this region, and to develop / maintain good conductivity and power system models for the same.

At times, even when such data is maintained and available, it is not trivial to obtain it for research as most power systems related data is considered to CEII, which has certain confidentiality requirements. Much of the GIC model data is relatively new from a power system studies perspective, such as substation locations, and might be a cause of concern for utilities in terms of sharing. Yet, validation research and model advancements cannot move forward unless data such as GICs and *B* measurements, as well as power system models including GIC model data are made available to the research community at large, with reasonable expectations of data security.

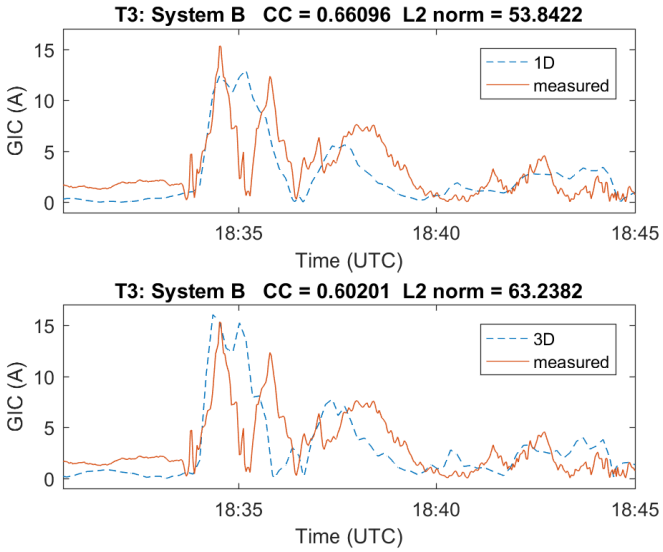

Figure 8. Comparison of Simulated and Measured GICs at T3 in System B

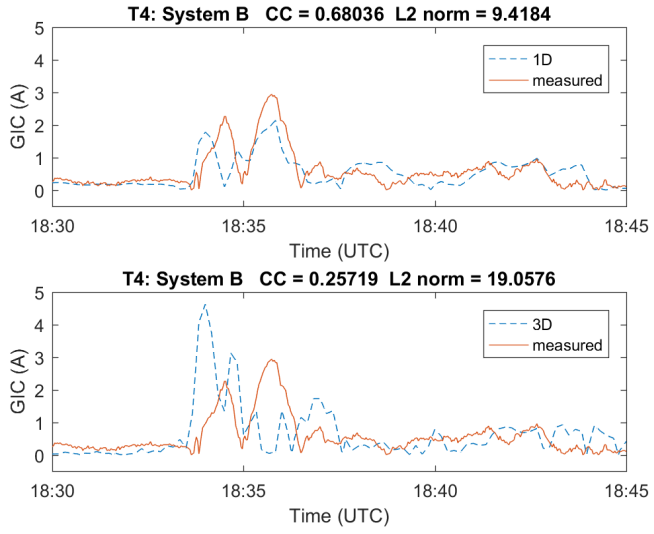

Figure 9. Comparison of Simulated and Measured GICs at T4

Mutual agreements can be made to protect and secure any data deemed sensitive, prior to and while doing any analysis. Anonymizing results or generalizing key conclusions in publications, working under non-disclosure agreements, conforming to cyber-security standards while handling the data, etc. are some of the tried and tested methods of achieving this. For instance, in this paper, more generalized conclusions could have been drawn on the conductivity structures if the same GMD event was studied across System A and B; data unavailability was an issue.

IV. Geophysical Observations

Because the time series in each case is derived from the same magnetic field inputs, the difference must be caused by the response of the earth conductivity to the source magnetic field. There are multiple geophysical differences between 1D and 3D-derived geoelectric field response, including spectral sensitivity and orientation differences, and uniformity of response. These will each be briefly discussed in this section as possibilities for the variation in correlation observed between events, locations, and conductivity type.

The 1D conductivity models and 3D EMTFs used to derive GIC estimates both represent geological conductivity structures that control the induced electric field response from a magnetic field fluctuation at the surface of the earth, and in both cases, these are given as a function of frequency. This means that, if there are differences in the spectral response of the two conductivity models, the 1D and 3D GIC estimates may be more sensitive to certain magnetic field frequencies. While the 1D models capture longer period response, 3D models are likely more correct on a local level. It is possibly that local differences in higher frequency response could cause differences between 1D and 3D-derived GIC estimates. In cases where the 1D models underperform, this could suggest the need for improvement in specific conductivity layers.

Geoelectric field orientation can be significantly different between 1D and 3D-derived response. Rotations in geoelectric field can significantly affect the coupling between the electric field and the transmission line, and appear in GIC estimates as intensity and phase estimation errors. It is likely that the scale size of the geophysical response greatly determines how much these differences actually affect GIC estimation, as long line integrations tend to smooth out smaller local effects. In addition, because the distance to the magnetometer used as input in many of these examples is great, there is significant uncertainty in the orientation of both the magnetic field driver and the geoelectric field response in both the 1D and 3D cases.

The uniformity of the geoelectric field response is likely another source of uncertainty in GIC estimation accuracy. Because, by definition, 1D models are uniform across large areas, they are much less affected by algorithm choices such as grid size and interpolation method. In the 3D response estimation, as more EMTF locations are added and bin size is decreased, any highly localized effects that may be present in

3D measurements become better resolved in spatial scale. In 3D-derived analyses, the more data that are used reduces the likelihood that a small-scale 3D geoelectric field response will affect surrounding areas.

Further analysis is needed to better understand the effect of these geophysical issues on GIC estimation. As magnetic field measurements become less sparse, 1D conductivity models improve, and advancements in 3D EMTF usage are made, we expect these comparisons to improve.

V. Summary and Future Work

In this paper, we evaluated some of the differences between the 1D conductivity and 3D EMTF based GIC simulations, by comparing them with GICs from actual GMD events. To this end, GIC simulations of large power system models were performed, using spatio-temporally varying electric fields that allow finer variations (for 3D) across large system footprints. Some of the good agreements between the simulated and actual GIC values demonstrate the GIC modeling state-of-the-art, and how far it has come since the uniform electric field assumption. The paper showed that models are, reasonably, able to reproduce the real world despite the various uncertainties in the GMD solution, with scope for improvement in areas such as conductivity modeling, magnetometer spacing, and certain power system model uncertainties. Performing more such validation studies of different events and across footprints will be a crucial aspect of improving these models and reducing uncertainties. The goal will be to gather enough sample points in order to make more general conclusions about the performance of these conductivity structures.

The purpose of this paper was not necessarily to conclude that one model is superior to the other, and hence it should be used in GIC studies. Rather it was to highlight the existing capabilities, limitations, and likely areas for improvement of each of these models. In addition, a major goal was to provide example simulation results as some sort of reference regarding what can be expected when these models are used for power system studies, as such comparisons are severely lacking in current literature. As seen, we are able to reproduce key properties of GIC time series such as peak values, or GIC activity measured through correlations, even from moderate events and using data and models riddled with uncertainties. The better the reproduction, the more trustworthy a model becomes. A validated, reliable system model can help ensure accurate GIC assessments and estimations. This should enable engineers to make sound operational and mitigation decisions, for a power grid facing a GMD. These are very pertinent and timely concerns, especially in light of the transmission planning standards [19] that are already in effect, which require periodic GMD hazard assessments along with maintaining system models for North American utilities on an ongoing basis.

VI. References

[1] V. D. Albertson and J. A. Van Baelen, "Electric and magnetic fields at the earth's surface due to auroral currents," *IEEE Trans. Power App. Syst.*, vol. PAS-89, pp. 578–584, Apr. 1970.

[2] D. H. Boteler, "Geomagnetically induced currents: Present knowledge and future research," *IEEE Trans. Power Del.*, vol. 9, pp. 50–58, Jan. 1994.

[3] D.H. Boteler, R.J. Pirjola, "Modeling Geomagnetically Induced Currents Produced by Realistic and Uniform Electric Fields," *IEEE Trans. on Power Delivery*, vol. 13, Oct. 1998, pp. 1303-1308.

[4] R. Horton, D. H. Boteler, T. J. Overbye, R. J. Pirjola, and R. Dugan, "A test case for the calculation of geomagnetically induced currents," *IEEE Trans. Power Del.*, vol. 27, pp. 2368–2373, Oct. 2012

[5] T. J. Overbye, K. S. Shetye, T. R. Hutchins, Q. Qiu, and J. D. Weber, "Power grid sensitivity analysis of geomagnetically induced currents," *IEEE Trans. on Power Systems*, vol. 28, no. 4, pp. 4821–4828, 2013.

[6] M. Kazerooni, H. Zhu, K. Shetye, and T. J. Overbye, "Estimation of geoelectric field for validating geomagnetic disturbance modeling," in *Power and Energy Conference at Illinois (PECI)*, Feb. 2013.

[7] V.D. Albertson, J.G. Kappenman, N. Mohan, and G.A. Skarbakka, "Load-Flow Studies in the Presence of Geomagnetically-Induced Currents," *IEEE Trans. on Power Apparatus and Systems*, vol. PAS-100, Feb. 1981, pp. 594-606.

[8] T. J. Overbye, T. R. Hutchins, K. Shetye, J. Weber, and S. Dahman, "Integration of geomagnetic disturbance modeling into the power flow: A methodology for large-scale system studies," in *Proc. 2012 North American Power Symp.*, Champaign, IL, USA, Sep. 2012.

[9] M. Kazerooni, H. Zhu, T. J. Overbye, "Transmission system geomagnetically induced current model validation," *IEEE Trans. on Power Sys.*, vol. 32, no. 3, pp. 2183-2192, 2017.

[10] "Regional Conductivity Maps," USGS. [Online]. Available: https://geomag.usgs.gov/conductivity/

[11] "Application Guide: Computing Geomagnetically-Induced Current in the Bulk-Power System, " NERC, Dec. 2013. [Online]. Available: http://www.nerc.com/comm/PC/Geomagnetic%20Disturbance%20Task%20Force%20GMDTF%202013/GIC%20Application%20Guide%202013-approved.pdf

[12] P. Fernberg, "One-Dimensional Earth Resistivity Models for Selected Areas of Continental United States & Alaska," EPRI, Palo Alto, CA, Technical Results (1026430), 2012.

[13] http://www.usarray.org/

[14] A. Schultz, G. D. Egbert, A. Kelbert, T. Peery, V. Clote, B. Fry, S. Erofeeva, and staff of the National Geoelectromagnetic Facility and their contractors," USArray TA Magnetotelluric Transfer Functions," (2006-2018) doi:10.17611/DP/EMTF/USARRAY/TA.

[15] Kelbert, A., G. Egbert, and A. Schultz, "Iris dmc data services products: Emtf, the magnetotelluric transfer functions," National Geoelectromagnetic Facility Technical Report, 2011.

[16] http://ds.iris.edu/spud/emtf

[17] J Gannon, A. B. Birchfield, K. S. Shetye, and Thomas J. Overbye, "A Comparison of Peak Electric Fields and GICs in the Pacific Northwest Using 1-D and 3-D Conductivity," *Space Weather*, vol. 15, no. 11, pp. 1535-1547, 2017.

[18] D. B. Percival, and A. T. Walden, "Wavelet Method for Time Series Analysis," Cambridge University Press, Cambridge, UK, 2000

[19] Transmission System Planned Performance for Geomagnetic Disturbance Events, NERC Std., TPL-007-2, Jun 2017.